Journal of Catalysis **192,** 119–127 (2000)
doi:10.1006/jcat.2000.2841, available online at http://www.idealibrary.com on IDEAL®

Gallioaluminosilicate Molecular Sieves with the Faujasite Structure

M. L. Occelli,* A. E. Schweizer,† C. Fild,‡ G. Schwering,‡ H. Eckert,‡ and A. Auroux§

*MLO Consultants, 6105 Black Water Trail, Atlanta, Georgia 30328; †Exxon R&D Laboratories, P.O. Box 2226, Baton Rouge, Louisiana 70821; ‡Institut fur Physikalische Chemie, Westfalische Wilhelms-Universitat Munster, Schlossplatz 7, D 48149 Munster, Germany; and §Institut de Recherches sur la Catalyse, CNRS, 2 Avenue A. Einstein, 69626 Villeurbanne, France

Received September 17, 1999; revised February 1, 2000; accepted February 4, 2000

Gallioaluminosilicate hydrogels with composition 0.1 Ga_2O_3 : 0.9 Al_2O_3 : 10 SiO_2 : 4.0 Na_2O : 150 H_2O were prepared using sodium aluminate, colloidal silica, and a soluble galliosilicate with composition Ga_2O_3 : 15 SiO_2 : 10 Na_2O : 400 H_2O as a source of gallia. The hydrothermal transformation of these gels at 95°C yields crystals with the faujasite structure when the crystallization reaction is performed in the absence of stirring and with the gmelinite structure (with minor amount of Pt) when crystallization is completed with stirring of the hydrogel. The crystallization time for Na(Ga,Al)Y can be decreased to 15 h from 48 h by raising the crystallization temperature to 110°C from 95°C. The calcined Na(Ga,Al)Y crystals have surface area in the 600 to 660 m^2/g range and, unless La-stabilized, suffer partial lattice degradation when, following an exchange with an NH_4NO_3 solution, the NH_4(Ga,Al)Y crystals are calcined at 500°C in air. This finding is clearly indicated by ^{27}Al, ^{71}Ga, and ^{29}Si MAS NMR spectroscopic results. The ^{29}Si NMR spectra of samples exchanged and calcined in the absence of La are poorly resolved and their quantitative analysis indicates substantial loss of Al and Ga from the faujasite framework. Consistent with this interpretation, ^{27}Al MAS NMR spectra reveal large amounts of octahedrally coordinated species in H(Ga,Al)Y. Moreover, the ^{71}Ga spectra show no evidence of tetrahedrally coordinated framework Ga. In contrast, the multinuclear NMR data of the H(Ga,Al,La)Y crystals indicate only minor Al and Ga losses from the framework, thus revealing the stabilizing influence of La. Thermodesorption of pyridine and microcalorimetry results with NH_3 have indicated that the La-stabilized H(Ga,Al,La)Y crystals have a more moderate acidity than the reference HY sample. Model fluid cracking catalyst (FCC)-containing H(Ga,Al,La)Y crystals are more active when cracking gas oil under microactivity testing conditions than similarly prepared FCC-containing HY-type zeolites and a reference equilibrium catalyst containing a rare-earth-stabilized HY, indicating that these crystals should be considered as acidic components in commercial FCC preparations. © 2000 Academic Press

Key Words: **galliosilicates; gallioaluminosilicates; Brønsted acidity; Lewis acidity; fluid cracking catalyst.**

INTRODUCTION

Today, zeolites with the faujasite structure remain the most technologically important molecular sieves since they are the main active components of fluid cracking catalysts (FCCs) and hydrocracking catalysts. When combined, these two processes are responsible for most of the transportation fluids produced in the industrialized world (1). A shift of 1% in the efficiency of oil conversion to liquid fuel is estimated to result in a saving of more than 22 million barrels of oil each year (2). Thus, it is not surprising that the petroleum engineer is continuously seeking to modify the properties of this type of zeolite knowing that small variations in its physicochemical properties can translate into large improvements in catalyst performance. In the past few years, the effects of Ga in zeolites have been the subject of numerous investigations (3–14). Of particular interest to refiners is the enhancement of aromatics yields from the aromatization of light paraffins over H(Ga-ZSM5) (3, 10). Furthermore, it has also been observed that Ga addition to the offretite framework decreases the hydrogen transfer properties of this zeolite during propylene conversion reactions (15). Thus Ga-containing zeolites with the faujasite structure could shift olefins distribution in products from gas oil conversion in a fluid cracking unit (FCCU) and may have similar effects also in zeolite-containing hydrocracking catalysts.

In a recent paper (16) it was shown that it is possible to rapidly synthesize GaY and that a postsynthesis ion exchange of Na with La ions drastically improves the crystals' thermal stability. Acid site strength and density in H(Ga,La)Y were found to be lower than those in HY-type crystals of the type used in FCC preparation (16). It is the purpose of this paper to describe the synthesis of some gallioaluminosilicates with the faujasite structure and report procedures to improve thermal and hydrothermal stability and to modify acidity properties.

EXPERIMENTAL

Synthesis

The source of gallium was obtained by adding water glass (PQ "N silicate" with ~29.8% SiO_2 and 9.07% Na_2O) to a sodium gallate solution prepared by dissolving Ga_2O_3 (99.99% pure, from Aldrich) in 50% NaOH; the Ga_2O_3/Na_2O molar oxide ratio was 5.58. After the

0021-9517/00 $35.00

solution was stirred at room temperature for ~24 h, a stable opalescent solution with composition Ga_2O_3 : 15 SiO_2 : 10 Na_2O : 400 H_2O was obtained. The shelf lifetime of this galliosilicate seeding solution is measured in months.

In a separate beaker an aluminosilicate gel with molar oxide composition Al_2O_3 : 11.1 SiO_2 : 4.44 Na_2O : 167 H_2O was prepared by reacting colloidal silica (Ludox AS-40) and sodium aluminate at room temperature. An aliquot of the seeding solution was then added to form a gallioaluminosilicate hydrogel with overall composition 0.1 Ga_2O_3 : 0.9 Al_2O_3 : 10 SiO_2 : 4.0 Na_2O : 150 H_2O; the crystallization reaction is completed after heating at 95°C (±1°C) for 48 h (or less).

Powder X-ray diffraction measurements were obtained using a Siemens D-500 diffractometer at a scan rate of 0.01°/step using 3 s/step monochromatic Cu$K\alpha$ radiation; CaF_2 was used as an internal standard for angle calibration.

Surface Area Analysis

Nitrogen sorption isotherms obtained at liquid nitrogen temperature were collected using a volumetric technique on a Micromeritics ASAP 2010 adsorption instrument equipped with version 3.0 software. Prior to analysis, samples weighing from 0.1–0.3 g were outgassed *in vacuo* at 400°C for at least 16 h. The total pore volume was derived from the amount of nitrogen adsorbed at a relative pressure close to unity ($p/P_o = 0.995$) by assuming that all the accessible pores were then filled with liquid nitrogen.

IR Analysis

IR spectra were obtained using a Nicolet 3600 spectrometer. Two spectra were obtained from each sample before the results were accepted as being representative of the zeolite sample under study. Spectra were acquired with a 2 cm^{-1} resolution (8192 data points) and apodized using the Happ-Genzel algorithm. Self-supporting wafers (4–8 mg/cm^2 in density) were prepared by pressing samples between 25-mm-diameter dies for 1 min at 6000–7000 lbs pressure. Prior to pyridine sorption, the wafers were mounted in an optical cell and degassed by heating at 200°C for 2 h at 10^{-3} Torr. The pyridine-loaded wafers were then heated (*in vacuo*) in the 200–500°C temperature range.

Microcalorimetry

Heat of adsorption of NH_3 was measured using a heat-flow C-80 Setaram microcalorimeter linked to a glass volumetric line. Successive doses of gas were sent onto the sample until a final equilibrium pressure of 133 Pa was obtained. The equilibrium pressure relative to each adsorbed amount was measured by means of a differential pressure gauge from Datametrics. The adsorption temperature was maintained at 150°C. Primary and secondary isotherms were collected at this temperature. All samples were outgassed overnight under vacuum at 400°C before calorimetric measurements were undertaken.

TABLE 1

Gas Oil Inspection

API gravity,°	26.2
ABP, °C	373.9
Nitrogen, wppm	569
Sulfur, wt%	1.19
Pour point, °C	18.3
Aniline point, °C	74.7
Conradson carbon, wt%	<0.05

Solid-State NMR

^{29}Si NMR spectra were recorded at 59.6 MHz on a modified Bruker CXP300 spectrometer. Samples were spun in cylindrical 7-mm zirconia rotors at spinning speeds near 4 kHz. In all cases, 90° pulses of 6-μs length and 30-s recycle delays were used. Chemical shifts were determined relative to tetramethylsilane as an external reference. ^{71}Ga and ^{27}Al MAS NMR spectra were obtained at 152.51 and 130.2 MHz, respectively, using a Bruker Avance (DSX) 500 spectrometer. Samples were spun in cylindrical 4-mm zirconia rotors at a spinning frequency of 12 kHz. The spectra were recorded with solid 45° pulses of 2-μs length and relaxation delays of 1 s. Resonance shifts are reported using liquid samples of 1 M aqueous solutions of $Ga(NO_3)_3$, and $Al(NO_3)_3$ as external reference standards.

Microactivity Testing

Microactivity testing (MAT) was performed on 80 × 150 mesh granules prepared by mixing 70% Georgia Kaolin with 30% zeolite powder. The resulting mixture was then pressed at 5000 lbs/min and the wafers thus produced were crushed and sized. MAT evaluation was conducted at a reactor temperature of 482°C, using an 80-s reaction time and a catalyst/oil ratio of 2.8. Gas oil inspection is given in Table 1. Prior to MAT, the granules were steam-aged for 5 h with 100% steam at 760°C and 1 atm. The reference equilibrium FCC has a surface area of 92 m^2/g and contains a rare-earth-stabilized HY-type zeolite with a unit cell of 2.435 nm; its rare-earth oxides content is 3.4%. In addition, this reference FCC contains 0.030 wt% Ni and 0.024 wt% V impurities.

RESULTS AND DISCUSSION

Synthesis

The hydrothermal transformation at 95°C of gallioaluminosilicate hydrogels with molar oxide composition 0.1 Ga_2O_3 : 0.9 Al_2O_3 : 10 SiO_2 : 4.0 Na_2O : 150 H_2O yielded crystals with the faujasite structure in the absence of stirring and gmelinite crystals (with minor amounts of Pt) in the presence of stirring (17). In the absence of Al , stirring caused the crystallization of gallium natrolite (16). The formation of Na(Ga,Al)Y is particularly sensitive to

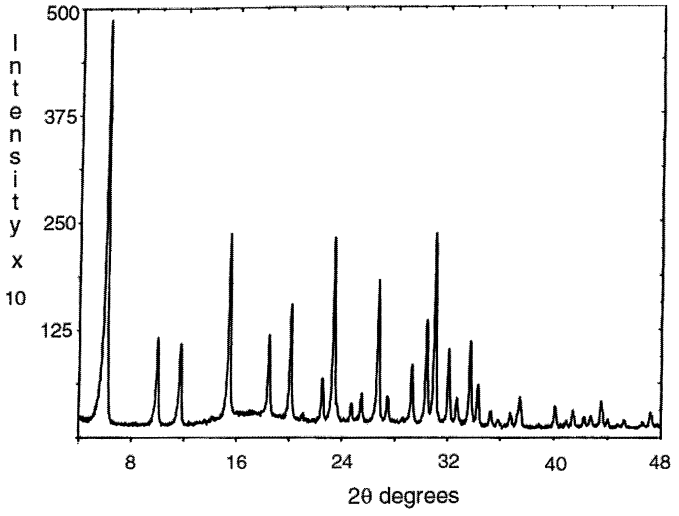

FIG. 1. Representative diffractogram of Na(Ga,Al)Y crystals after drying at 100°C.

temperature. In fact, the crystallization time decreases to 15 h from ~48 h when the temperature is raised to 110°C from 95°C. A representative XRD pattern is given in Fig. 1; composition and surface area data are shown in Table 2.

Na(Ga,Al)Y can also be synthesized from the same hydrogel prepared using sodium gallate instead of galliosilicate solutions; in this case, longer crystallization times are required. In general, these crystallization reactions are not stoichiometric and the crystals' silica-to-gallia and -alumina ratio is always lower than that of the parent hydrogel (Table 2). Removal of Na ions with a 1 M NH_4NO_3 solution and calcination at 500°C decreases the $\%Na_2O$ to 0.76 from 11.6 and the surface area to 448 m^2/g from 659 m^2/g, indicating a partial degradation of the Na(Al,Ga)Y crystals' structure. Thus, as already reported for other zeolites such as offretite (18) and Beta (19), the introduction of Ga atoms decreases the faujasite framework thermal stability.

As observed in Al-free GaY crystals (16), the stability of Ga-containing faujasites can be drastically improved by preceding the NH_4-exchange step by a La-exchange reaction in a 0.33 M $LaCl_3$ solution followed by calcination in air at 440°C/10 h; see Table 2. The properties of H(Ga,Al,La)Y and of similarly (16) prepared H(Ga,La)Y are shown in Table 2. In this table, reference galliosilicates such as GaY and H(Ga,La)Y have been included for comparison purposes (16). The calcination step for the La-exchanged crystals is needed to prevent La losses during the replacement of residual Na with NH_4 ions. Similar results have been observed when reacting calcined, rare-earth exchanged Y (CREY) crystals, with NH_4NO_3 solutions to reduce the $\%Na_2O$ to 0.11 from 3.40 without significantly affecting the CREY rare-earth metal content (20). It is believed that La ions become part of the zeolite framework by forming two –La(OH)– bridges in the sodalite cages that impart stability to the faujasite structure (21).

TABLE 2

Composition and Surface Area of Some Ga-Containing Faujasites

Sample	SA, m^2/g	Molar oxide composition				
		Ga_2O_3	Al_2O_3	SiO_2	Na_2O	La_2O_3
NaGaY	515	1.0	—	4.37	1.09	—
H(Ga,La)Y	503	1.0	—	4.40	0.12	0.25
Na(Ga,Al)Y	659	0.1	0.90	5.21	0.99	—
H(Ga,Al)Y	448	0.090	0.91	5.25	0.05	—
H(Ga,Al,La)Y	610	0.093	0.907	5.00	0.06	0.23

Note. Data for Al-free NaGaY and H(Ga,La)Y were obtained from Ref. (16).

^{29}Si MAS NMR Results

The ^{29}Si MAS NMR spectra of the different gallioaluminosilicates under study are compared in Fig. 2. As expected, the ^{29}Si spectra for Na(Ga,Al)Y samples yield a typical pattern of signal attributable to T(1Si,3*M*), T(2Si,2*M*), T(3Si,1*M*), and T(4Si,0*M*) units, respectively; M = Al, Ga (22, 23). The ^{29}Si NMR spectrum in Fig. 2A for Na(Ga,Al)Y closely resembles the one obtained for (Na,Al)Y (16) and

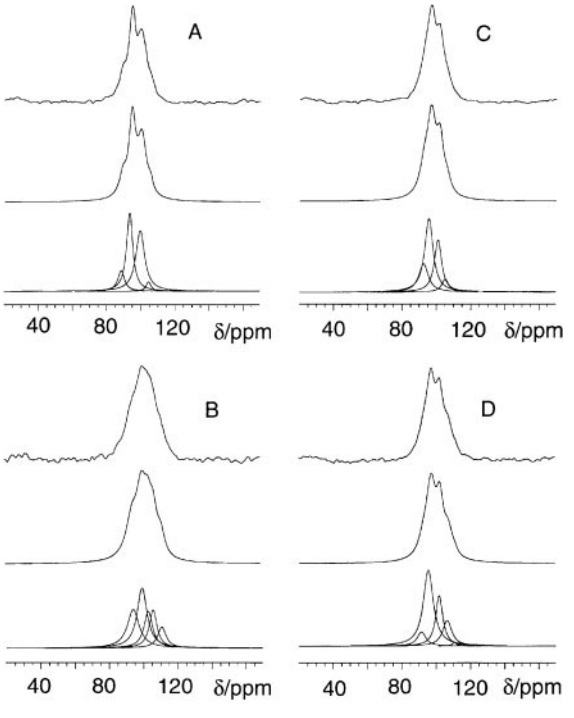

FIG. 2. ^{29}Si NMR spectra for Na(Ga,Al)Y prepared from seeded hydrogels (A) before and (B) after NH_4 exchange and calcination to form H(Ga,Al)Y crystals, (C) after La and NH_4 exchange to form NH_4(Ga,Al,La)Y crystals, and (D) after La and NH_4 exchange and calcination to form H(Ga,Al,La)Y crystals. In each part, the top trace is the experimental spectrum, the middle trace corresponds to a simulation, and the bottom trace shows the individual contributions of the T[*n*Si,(4-*n*)*M*] sites.

TABLE 3

^{29}Si Chemical Shifts for Several Gallioaluminosilicates

Sample	Chemical shift (ppm)				Si/M^a	
	T(1Si,3Al)	T(2Si,2Al)	T(3Si,1Al)	T(4Si,0Al)	NMR	Chem.
1. Na(Ga,Al)Y	88.8	94.1	99.9	105.0	2.50	2.60
2. H(Ga,Al)Y	—	94.2	99.7	106.7	4.0[c]	2.62
			103.4	111.1		
3. NH_4(Ga,Al,La)Y	92.8	96.7	101.7	105.9	2.25	—
4. H(Ga,Al,La)Y	92.5	96.6	101.8	107.1	2.29	2.50
				110.9		
5. H(Ga,Al,La)Y[b]	92.4	97.0	102.2	107.1	2.62	2.50

[a] M = Ga + Al.
[b] Repeat with shorter intermediate calcination time.
[c] Estimated value.

shows four sites corresponding to 0, 1, 2, and 3 Al or Ga neighbors. The Si/(Ga + Al) ratio is 2.50, in agreement with the value of 2.58 obtained from chemical analysis data, Table 2. Changing the batch size from 0.5 *l* to 5.0 *l* has little effect on the crystals' properties. Large batches of Na(Ga,Al)Y can be reproduced with ease, yielding crystals with similar properties as well as ^{29}Si NMR spectra.

The ion-exchange reaction of Na(Ga,Al)Y with NH_4NO_3 solutions and calcination at 500°C degrades the crystal quality and the ^{29}Si NMR spectrum for H(Ga,Al)Y reveals very poor resolution. The fairly featureless spectrum in Fig. 2B can be deconvoluted into five lineshape components. Of these, the two upfield components at −111.2 and −106.7 ppm are T(4Si,0*M*) silicon sites. The peak at −111.2 ppm may be due to extraframework amorphous silica generated by lattice degradation (24). Two additional components at −103.44 and −99.7 ppm occur within the T(3Si,1*M*) region, while the most downfield component located at −94.2 ppm is assignable to a T(2Si,2*M*) environment. From the lineshape deconvolution an Si/*M* ratio of 4 (±0.5) can be estimated. In this case, the error is large due to the poor resolution in the spectrum. The discrepancy between Si/*M* values from NMR and chemical analysis can be safely attributed to demetalation of the faujasite structure.

Structural stability can be improved by the addition of lanthanides. The ^{29}Si NMR spectrum in Fig. 2C for NH_4(Ga,Al,La)Y is quite similar to the one in Fig. 2A, indicating that the ammonium exchange step after La addition does not affect framework structure nor ^{29}Si chemical shifts. Only the extent of line broadening is somewhat increased, indicating a higher degree of structural disorder. Calcination in air at 500°C generates H(Ga,Al,La)Y crystals with a ^{29}Si NMR spectrum that still has an appearance similar to that of the starting Na(Ga,Al,)Y; see Figs. 2A–2D. Clearly, the spectrum of the La-stabilized sample shows significantly improved resolution compared to that of the La-free H(Ga,Al)Y crystals in Fig. 2B. From the ^{29}Si NMR spectrum the Si/*M* ratio computes to 2.62, indicating that there has been only a minor loss of *M* species from the faujasite framework after the calcination step, Table 3. Metal losses from the framework can be minimized by reducing the intermediate calcination step of the La-exchanged crystals to 2 from 10 h. In these crystals, formation of extraframework silica (peak near −111 ppm) has been suppressed and the Si/*M* ratio of 2.25 closely resembles that of the parent material; see Table 3. In agreement with XRD results and SA data, the ^{29}Si spectra in Figs. 2B–2D illustrate the increased structural stability resulting from lanthanum incorporation in crystalline gallioaluminosilicates with the faujasite structure.

^{27}Al and ^{71}Ga MAS NMR Results

Figures 3 and 4 summarize the ^{27}Al and ^{71}Ga MAS NMR spectra of the samples studied. For the air-dried

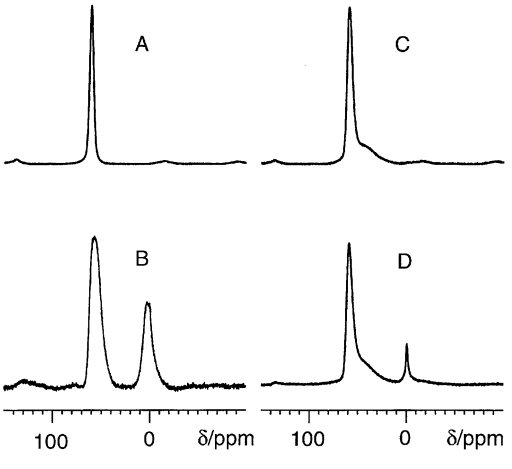

FIG. 3. ^{27}Al MAS NMR spectra for Na(Ga,Al)Y prepared from seeded hydrogels (A) before and (B) after NH_4 exchange and calcination to form H(Ga,Al)Y crystals, (C) after La and NH_4 exchange to form NH_4(Ga,Al,La)Y crystals, and (D) after La and NH_4 exchange and calcination to form H(Ga,Al,La)Y crystals.

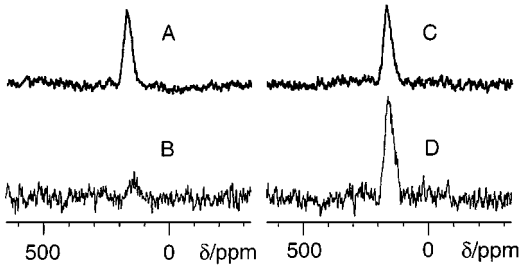

FIG. 4. ^{71}Ga NMR spectra at 7.04 T for Na(Ga,Al)Y prepared from seeded hydrogels (A) before and (B) after NH_4 exchange and calcination to form H(Ga,Al)Y crystals, (C) after La and NH_4 exchange to form NH_4(Ga,Al,La)Y crystals, and (D) after La and NH_4 exchange and calcination to form H(Ga,Al,La)Y crystals.

Na(Ga,Al)Y sample, the spectra in Figs. 3A and 4A reveal the sole presence of tetrahedral species, explaining the excellent agreement between Si/*M* values from ^{29}Si NMR data and from chemical analysis. Extraframework metal atoms were not observed in any of the Na(Ga,Al)Y crystals that had been dried at 100°C. After direct exchange of charge-compensating Na with NH_4 ions and subsequent calcination of the sample the ^{27}Al MAS NMR spectrum reveals loss of resolution and a significant amount of octahedral extraframework Al species is formed; see Fig. 3B. A very weak and broad gallium signal was observable in this sample, indicating the nearly complete removal of gallium from the framework, Fig. 4B. Most likely, the extraframework Ga species is so strongly disordered that the signal is broadened into the baseline by a wide distribution of nuclear electric quadrupolar coupling constants. As already anticipated from the poorly resolved ^{29}Si NMR spectrum in Fig. 2B, these results confirm the occurrence of considerable lattice degradation in these crystals.

In contrast, if the Na(Ga,Al)Y crystals are first La-exchanged and calcined before a second ion exchange with NH_4 to remove residual Na ions, the calcination of NH_4(Ga,Al,La)Y has only a minor effect on crystal properties. As a result, crystallinity and SA remain high, Table 2. Nevertheless, the ^{27}Al spectrum of the H(Ga,Al,La)Y sample thus produced shows a minor amount of more highly coordinated aluminum. The broad and weak resonance centered near 35 ppm in Figs. 3C and 3D is attributed to five-coordinate aluminum species. In Fig. 3D, the fairly sharp peak near 2 ppm reflects instead octahedrally coordinated aluminum species. The same trend is evident in the ^{71}Ga MAS NMR spectra shown in Figs. 4C and 4D. Only tetrahedral gallium is clearly detected but with somewhat lower intensity compared to that of the air-dried Na(Ga,Al)Y sample. This loss of signal intensity is the result of a minor lattice degradation suffered by these crystals. Nevertheless, the sample's crystallinity remains high and its SA of 610 m^2/g is only slightly lower than that of the reference HAlY; see Table 2.

IR Results

Before pyridine sorption, the H(Ga,Al,La)Y spectrum in the OH stretching region consists of three bands; see Fig. 5A. In addition to the high-frequency (hf) band assigned to terminal Si–OH groups, the spectrum contains an intense band centered near 3528 cm^{-1} overlapping a less intense one centered near 3637 cm^{-1}. After pyridine sorption, the 3528 cm^{-1} band shifts to higher wavenumbers. However, when the degassing temperature is monotonically increased to 500°C from 200°C, this band broadens, undergoes a minor decrease in intensity, and shifts toward its original position, Fig. 5A. In contrast, the band at 3637 cm^{-1} readily interacts with pyridine, and at 200°C it is no longer visible. This band shifts to lower wavenumbers and it reappears at $T > 300$°C, that is, after pyridine begins to be thermally removed from the crystals. However, its original intensity is not restored, probably because of dehydroxylation reactions, Fig. 5A.

Although the ^{27}Al MAS NMR spectrum for H(Ga,Al,La)Y indicates the presence of Al(VI) species, IR bands near 3660 cm^{-1} attributed to extraframework metal atoms (25, 26) are not visible in this sample. Furthermore, bands in the 3520–3540 cm^{-1} region seen in rare-earth (RE)-containing faujasite crystals (25, 26) are also noticeably absent in the H(Ga,Al,La)Y spectrum; see Fig. 5A. Bands in this region have been assigned to hydroxyls (such as –LaOH–) associated with RE ions (21, 25, 27). It has been proposed (21) that the hydrolysis of RE ions (such as La) forms $-RE(OH)_2$ and –RE(OH)– groups that stabilize the sodalite units. The protons generated from the hydrolysis reaction form new *M*–OH groups believed to be responsible for the acidic band in the 3635–3645 cm^{-1} region; see Fig. 5A.

The infrared bands of pyridine of interest to this study are the C–H and N–H stretching frequencies as well as the C–C and the C–N stretching frequencies at 1590–1660 cm^{-1} and near 1500 cm^{-1} (28). In Fig. 5A, the low-frequency (lf) band at 3237 cm^{-1} has been attributed to the pyridine's =N–H groups (28). The intensity of this band monotonically decreases with increasing the degassing temperature and almost disappears at 500°C. IR spectra showing the C–C and C–N stretching vibration of chemisorbed pyridine on these crystals are shown in Fig. 5B. Bands near 1540 cm^{-1} represent protonation of pyridine by B-sites and the presence of coordinatively bonded pyridine on L-sites is shown by bands near 1450 cm^{-1} (29). In Table 4, Brønsted (B) and Lewis (L) acid site density as a function of degassing temperature has been obtained by dividing the integrated absorbance (in the 1563–1523 cm^{-1} region and in the 1468–1438 cm^{-1} region) by the sample density.

In contrast to that observed for H(Ga,La)Y and in agreement with HY (LZY-82) results (20), acidity in H(Ga,Al,La)Y is mainly of the B-type and in the 200–500°C temperature range the B/L ratio remains greater than one,

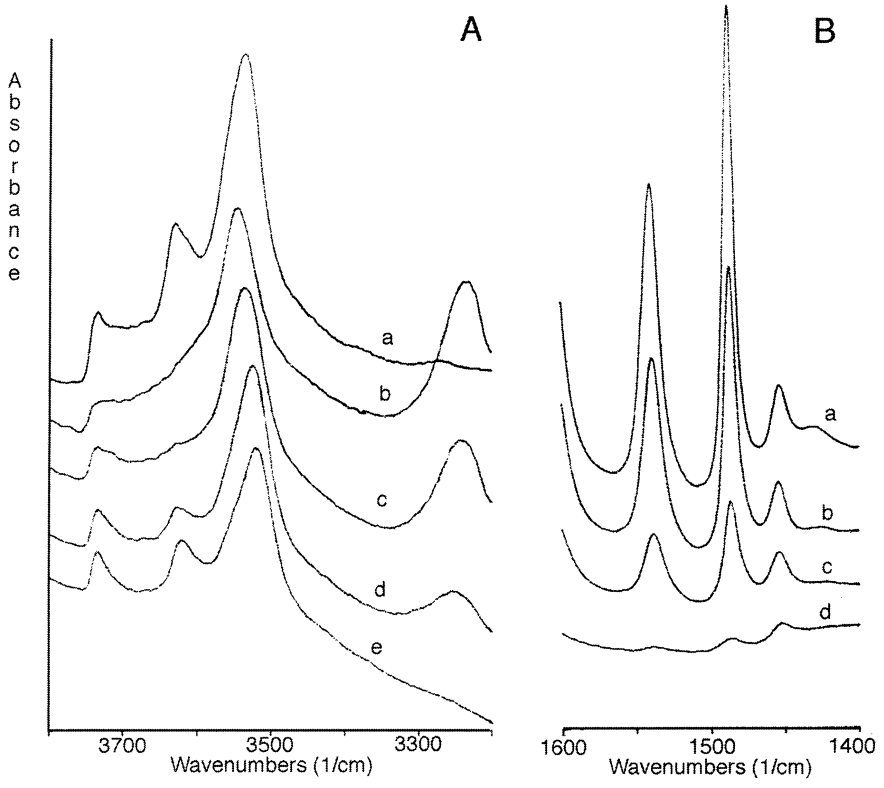

FIG. 5. Infrared spectra of chemisorbed pyridine on H(Ga,Al,La)Y: (A) The OH stretching region. Samples have been degassed at 200°C (a) and then exposed to pyridine and degassed at: (b) 200, (c) 300, (d) 400, and (e) 500°C. (B) The C–C stretching region. Samples have been degassed at 200°C and then exposed to pyridine and degassed at: (a) 200, (b) 300, (c) 400, and (d) 500°C.

Fig. 5B. Pyridine desorption data in Table 4 indicate that, in all the samples examined, thermal desorption is more facile from B-sites than from L-sites and that, in the presence of La, the isomorphous substitution of Al by Ga as in H(Ga,Al,La)Y, has only minor effects on acid site strength and distribution. Acidity is weakest in Al-free, H(Ga,La)Y crystals (16) and drastically increases after removal of most of the charge-compensating Na ions in (Al,Ga)Y with La and NH_4 ions, Table 4. Introduction of La into the (Ga,Al)Y framework increases the relative distribution of B- and L-sites and the B/L acid site ratio almost doubles in value; see Table 4. However, the new sites are not as strongly acidic as those observed in the reference HY (LZY-82) crystals (20). The more moderate acidity of H(Ga,Al,La)Y could have an effect on the hydrogen transfer properties of these crystals.

Microcalorimetry

The sorption isotherms in Fig. 6 and the data in Table 2 indicate that the number of sites available to NH_3 chemisorption in these Ga-containing faujasites increases in the order H(Ga,La)Y < H(Ga,Al)Y < HY (LZY-82) < H(Ga,Al,La)Y. Not shown are secondary sorption isotherms, that is, sorption isotherms for samples after NH_3 adsorption and degassing in vacuum at 150°C. By subtracting

TABLE 4

Pyridine Chemisorption Data for Several Ga-Containing Faujasites and Reference HY, Calcined at 540°C

	(H,Al)Y			H(Ga,La)Y(16)			H(Ga,Al)Y			H(Ga,Al,La)Y		
T (°C)	B	L	B/L	B	L	B/L	B	L	B/L	B	L	B/L
200	0.59	0.13	4.54	0.25	0.92	0.27	1.09	0.33	3.30	0.84	0.13	6.46
300	0.47	0.09	5.22	0.08	0.85	0.09	0.92	0.25	3.68	0.51	0.10	5.10
400	0.27	0.05	5.40	—	0.60	—	0.50	0.25	2.00	0.16	0.08	2.00
500	0.10	0.03	3.33	—	0.27	—	0.10	0.24	0.42	[a]	[a]	[a]

Note. The samples, composition is given in Table 2.
[a] Could not be integrated with accuracy.

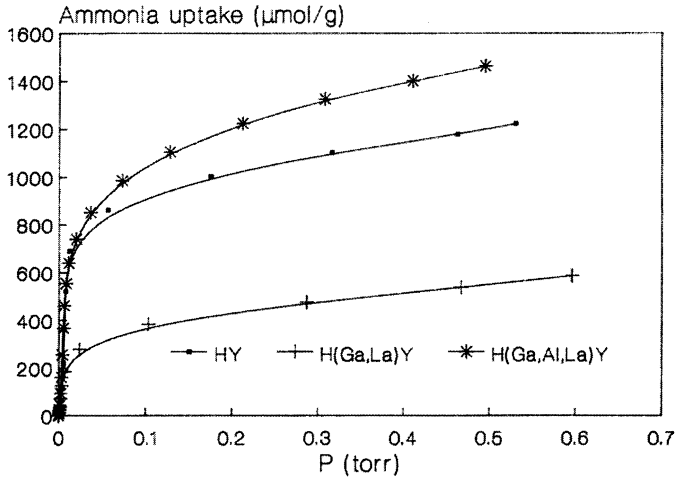

FIG. 6. Ammonia sorption isotherms for HY (LZY-82), H(Ga,Al)Y, and H(Ga,Al,La)Y crystals.

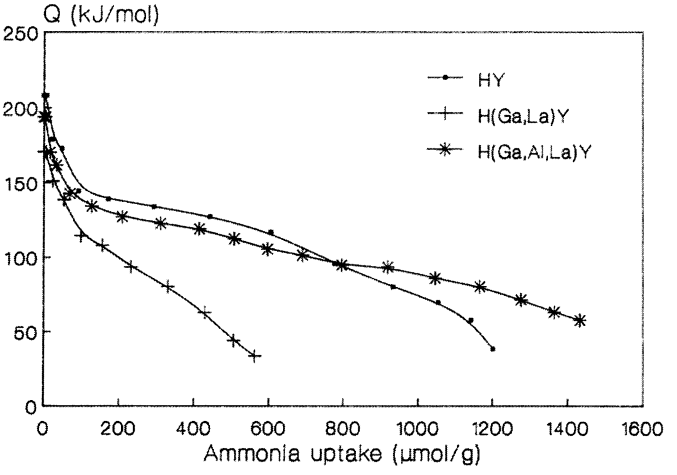

FIG. 7. Differential heats profiles as a function of ammonia uptake for HY (LZY-82), H(Ga,Al)Y, and H(Ga,Al,La)Y crystals.

the adsorbed volume of the secondary isotherms from that of the primary isotherms at the same equilibrium pressure ($p = 0.2$ Torr), it is possible to obtain V_{irr}, that is, the irreversibly chemisorbed volume of NH_3. This value is believed to represent the total number of strong (B + L) acid sites present in the solids under study (30, 31).

Initial heats (In. H), integral heat (Int. H., the total heat evolved at $p = 0.2$ Torr), and the total and irreversibly chemisorbed NH_3, together with the site population with a given strength, are given in Table 5. These results highlight the comparable acidic properties (as determined by NH_3 chemisorption) between the calcined HAlY (LZY-82) and the La-stabilized H(Ga,Al,La)Y crystals. The strength of the strongest sites increases, as determined from initial heat data, from 171 kJ/mol in the Al-free H(Ga,La)Y to 194 kJ/mol in H(Ga,Al,La)Y and to 208 kJ/mol in the Ga-free reference HAlY crystals. The main difference between the faujasites under study is represented by the larger number of sites (B+L) with moderate (<100 kJ/mol) acidity that exist in H(Ga,Al,La)Y and by the larger number of strong (>150 kJ/mol) acid sites (B + L) that are present in the reference HY (LZY-82) sample; see Table 5.

TABLE 5

Ammonia Chemisorption Data at 150°C ($p = 0.2$ Torr)

Sample	In. H, kJ/mol	Int. H, J/g	NH_3 (μmol/g) V_T	NH_3 (μmol/g) V_{irr}	kJ/mol <100	kJ/mol 100–150	kJ/mol >150
1. H(Ga,La)Y	171	43	431	217	233	171	27
2. H(Ga,Al,)Y	180	66	616	399	282	287	47
3. H(Ga,Al,La)Y	194	132	1206	681	495	655	56
4. HY (LZY-82)	208	122	1020	680	279	657	84

Note. Population of sites with given strength is in μmol NH_3/g.

Differential heat profiles in Fig. 7 show that as Al is replaced by Ga, acid site strength as well as acid site density decreases. Acid site strength is lowest in Al-free H(Ga,La)Y (16) and increases in the order H(Ga,La)Y < H(Ga,Al)Y < H(Ga,Al,La)Y < HY (LZY-82) in agreement with initial heats results. The reference HY contains a small population of sites with strength in the 150–220 kJ/mol range attributed to extraframework Al(VI) (32–34); formation of Al(VI) species in the calcined HY (LZY-82) has been observed by NMR (24). As ammonia coverage increases above 180 μmol of NH_3/g, a population of sites with strength near 140 kJ/mol, representing the interaction of ammonia with bridging hydroxyls, appears (32–36). In H(Ga,Al,La)Y, the loss in acid strength is compensated by an increase in population of sites with moderate (near 100 kJ/mol) strength. These sites have been attributed to the interaction of ammonia with La species in H(Ga,Al,La)Y crystals.

Microactivity Test Results

Differences in microactivity between catalysts containing the reference HY (LZY-82) zeolite and H(Ga,Al,La)Y are attributed mainly to crystallinity and acidity modifications in the faujasite crystals during steam aging with 100% steam at 760°C for 5 h. During steam aging, the unit cell dimension for H(Ga,Al,La)Y, with $Ga_2O_3/[Ga_2O_3 + Al_2O_3] = 0.1$, decreased to 2.448 nm from 2.475 nm in the dried FCC. This contraction is similar to that experienced by the Kaolin/HY mixture. Thermal and hydrothermal stability in H(Ga,Al,La)Y decreases with increasing Ga content, and when the $Ga_2O_3/[Ga_2O_3 + Al_2O_3]$ molar oxide ratio is increased to 0.2 from 0.1 the crystals become hydrothermally unstable.

Results in Table 6 indicate that the stable Kaolin/H(Ga,Al,La)Y mixture converts more of the SO fraction to generate greater gasoline, and similar LCGO, yields

TABLE 6

Microactivity Test Results for Kaolin (80 × 150 Mesh) Granules Promoted with 30 wt% HY or 30 wt% H(Ga,Al,La)Y Crystals

	HY	H(Ga,Al,La)Y	Equil. FCC
Conversion (wt% ff)	62.0	73.9	72.4
Gasoline (wt% ff)	44.2	46.8	48.8
LCGO (wt% ff)	20.9	17.7	18.9
SO (wt% ff)	17.1	8.4	8.7
$\sum C_2^=–C_4^=$ (wt% ff)	4.07	4.39	4.28
$\sum C_2–C_4$ (wt% ff)	2.35	3.72	3.49
$\sum C_2^=–C_4^= / \sum C_2–C_4$	1.73	1.18	1.22
Methane (wt% ff)	0.047	0.068	0.060
Hydrogen (wt% ff)	0.066	0.10	0.086
Coke (wt% ff)	1.50	3.73	2.75

Note. Conversion has been defined as 100 -% mid-distillate yields.

as the Kaolin/HY granules. Because of the large difference in cracking activity between the two model FCCs, the $\sum[C_2^=–C_4^=]/\sum[C_2–C_4]$ ratios in Table 6 cannot be used to compare the H transfer activity of HY and H(Ga,Al,La)Y crystals. The gasoline/conversion and the coke/conversion ratios of 0.63 and 0.05 are in agreement with the values of 0.67 and 0.04 observed for the equilibrium FCC used to calibrate the MAT unit. Thus, the two-step ion exchange with La and NH_4 ions generates H(Ga,Al,La)Y crystals with a more moderate acidity than HY and with a hydrothermal stability that should encourage catalyst makers and refiners to consider these crystals as possible cracking components of FCCs.

SUMMARY AND CONCLUSION

Crystalline gallioaluminosilicates with the faujasite structure have been synthesized by heating at 95°C/48 h without stirring, a hydrogel with composition 0.1 Ga_2O_3 : 0.9 Al_2O_3 : 10 SiO_2 : 4.0 Na_2O : 150 H_2O in which gallium was added as a soluble galliosilicate with composition Ga_2O_3 : 15 SiO_2 : 10 Na_2O : 400 H_2O. As observed in the synthesis of GaY, the crystallization product of these gels is controlled by synthesis conditions. In fact, at 95°C, stirring during crystallization causes gmelinite formation, while increasing the crystallization temperature to 110°C from 95°C decreases crystallization times by about 33 h. The replacement of Na with NH_4 ions and calcination induce a partial degradation of the faujasite structure unless La ions are introduced before the NH_4-exchange and calcination step. It is believed that La ions become part of the zeolite framework by forming two –La(OH)– bridges in the sodalite cages that *help impart* stability to the faujasite structure (21). During thermal and hydrothermal treatments, proton attack causes the rupture of Si–O–*M* bonds and the collapse of the faujasite framework; M = Al, Ga. The presence of cross-linking lanthanide bridges and the presence of less acidic La acid sites will hinder proton attack, thus increasing lattice stability.

^{71}Ga and ^{27}Al MAS NMR results indicate that the pristine Na(Al,Ga)Y crystals do not contain extraframework Ga or Al species. ^{29}Si MAS NMR spectra are in agreement with published results for (Na,Al)Y and yield Si/*M* molar ratios consistent with chemical analysis. The H(Ga,Al)Y spectra are considerably less resolved than the spectrum for Na(Ga,Al)Y because of severe crystal degradation during the NH_4-exchange and calcination step. In contrast, spectra of the La-stabilized H(Ga,Al,La)Y are much closer to the spectrum of the parent Na(Ga,Al)Y indicating only a minor degree of lattice degradation.

FTIR results from pyridine thermodesorption in the 200 to 500°C temperature range have indicated that the partial replacement of Al with Ga in the La-containing faujasite framework increases B acid site density at the expense of strength and at 500°C only trace amounts of pyridine are retained on H(Ga,Al,La)Y. These results are in agreement with published data, indicating that the isomorphous substitution of Al with Ga in zeolites reduces acid site strength and affects acid site distributions (16, 18, 19).

Microcalorimetry experiments with NH_3 as the probe molecule have demonstrated that the acidic properties of the faujasite framework can be modified by changing the framework composition. Acidity in these crystals can be altered without sacrificing thermal stability, by replacing framework Al with Ga as in H(Ga,Al,La)Y. In summary, the total volume of NH_3 sorbed and the number of acid sites (B + L) with moderate strength as well as integral heats of adsorption are greater in H(Ga,Al,La)Y than in HY(LZY-82). Because of its excellent thermal stability, unique acidity properties, and cracking activity during gas oil conversion under MAT conditions, H(Ga,Al,La)Y crystals should be considered as an acidic component in FCCs preparation.

ACKNOWLEDGMENTS

This work has been supported in part by NATO collaborative grant CRG-971497 to M.L.O. and H.E. Special thanks are due to E. Rivette, M. Bell, and Dr. P. Ritz for XRD and IR data. H.E., C.F., and G.S. acknowledge support from the Wissenschaftsministerium Nordrhein-Westfalen.

REFERENCES

1. Rhodes, A. K., *Oil Gas J.* December 18, 41 (1995).
2. Federal Register, Vol. 57, No. 13, January 21, 1992.
3. Meriaudeau, P., and Naccache, C., *J. Mol. Catal.* **50**, L7 (1989).
4. Kanazirev, V., Price, G. L., and Dooley, K. M., *J. Chem. Soc., Chem. Commun.* 712 (1990).
5. Schultz, P., and Baems, M., *Appl. Catal.* **78**, 15 (1991).
6. Corma, A., Goberna, C., Lopez Nieto, J. M., Paredes, N., and Perez, M., *in* "Zeolite Chemistry and Catalysis" (P. A. Jacobs, et al., Eds.), p. 409. Elsevier, Amsterdam, 1991.
7. Stakheev, A. Yu., Khodakov, A. Yu., L. M., Kazansky, V. B., and Minachev, Kh. M., *Zeolites* **12**, 866 (1992).

8. Yao, J., Le van Mao, R., Kharson, M. S., and Dufresne, L., *Appl. Catal.* **65**, 670 (1992).
9. Bandiera, J., and Taarit, Y. B., *Appl. Catal.* **76**, 199 (1991).
10. Inui, T., Makino, Y., Okazumi, F., and Miyamoto, A., *J. Chem. Soc., Chem. Commun.* 571 (1986).
11. Meriaudeau, P., and Naccache, C., *J. Mol. Catal.* **59**, L31 (1990).
12. Iglesia, E., Baumgartner, J. E., and Price, G. L., *J. Catal.* **134**, 549 (1992).
13. Gnep, N. S., Doyemet, J. Y., Seco, A. M., Ribeiro, F. R., and Guisnet, M., *Appl. Catal.* **43**, 155 (1988).
14. Bayense, C. R., and van Hooff, J. H. C., *Appl. Catal. A* **79**, 127 (1991).
15. Dai, E., Tsang, C. M., Petty, R. H., Somervell, M., Williamson, B., and Occelli, M. L., *in* "Progress in Zeolite and Micxroporous Materials" (H. Chon, S.-K. Ihm, and Y. S. Uh, Eds.), Studies in Surface Science and Catalysis Vol. 105B, pp. 981–987. Elsevier, Amsterdam, 1996.
16. Occelli, M. L., Eckert, H., Auroux, A., and Iyer, P. S., *Micropor. Mesopor. Mater.* **34**, 1, 15–22 (2000).
17. Occelli, M. L., U.S. Patent 5,053,213 (1991).
18. Occelli, M. L., Eckert, H., Hudalla, C., Auroux, A., Ritz, P., and Iyer, P. S., *in* "Progress in Zeolite and Microporous Materials " (H. Chon, S.-K. Ihm, and Y. S. Uh, Eds.), Studies in Surface Science and Catalysis Vol. 105C, pp. 1981–1987. Elsevier, Amsterdam, 1996.
19. Occelli, M. L., Auroux, A., and Eckert, H., *Micropor. Mesopor. Mater.* **30**, 219–232 (1999).
20. Occelli, M. L., and Ritz, P., *Appl. Catal. A: Gen.* **183**, 53–59 (1999).
21. Rabo, J. A., Angell, C. L., and Schoomaker, V., *in* "Proceedings 4th International Congress on Catalysis, Moscow, 1968" (B. A. Kazansky, Ed.), Adler, New York, 1968.
22. Thomas, J. M., Klinowski, J., Ramdas, S., Anderson, M. W., Fyfe, C. A., and Gobbi, G. C., *in* "Intrazeolite Chemistry" (G. Stucky, Ed.), ACS Symposium Series 218, p. 158, Am. Chem. Soc., Washington, DC, 1983.
23. Melchior, M. T., *in* "Intrazeolite Chemistry" (G. Stucky, Ed.), ACS Symposium Series 218, p. 243. Am. Chem. Soc., Washington, DC, 1983.
24. Occelli, M. L., *in* "Catalysis in Petroleum Refining and Petrochemical Industries" (M. Absi-Halabi, J. Beshara, H. Qabazard, and A. Stanislaus, Eds.), pp. 217–247. Elsevier, Amsterdam, 1996.
25. Scherzer, J., and Bass J. L., *J. Catal.* **46**, 100 (1977).
26. Jacobs, P. A., and Uytterhoeven, J. B., *J. Chem. Soc., Faraday Trans. 1* **13**, 373 (1973).
27. Beyerlein, R. A., McVicker, G. B., Yacullo, L. N., and Ziemiak, J. J., *J. Phys. Chem.* **92**, 1967 (1988).
28. Klingsberg, E., "Pyridine and its derivatives. Part I," p. 11. Interscience, New York, 1960.
29. Parry, E. P., *J. Catal.* **2**, 371–379 (1963).
30. Auroux, A., *in* "Catalyst Characterization: Physical Techniques for Solid Materials" (B. Imelik and J. C. Vedrine, Eds.), Chap. 22. Plenum, New York, 1994.
31. Auroux, A., *Topics Catal.* **4**, 71–89 (1997).
32. Auroux, A., and Ben Taarit, Y., *Thermochim. Acta* **122**, 63 (1987).
33. Shi, Z. C., Auroux, A., and Ben Taarit, Y., *Can. J. Chem.* **66**, 1013 (1983).
34. Cardona-Martinez, N., and Dumesic, J. A., *J. Catal.* **125**, 427 (1990).
35. Kuehne, M. A., Babitz, S. M., Kung, H. H., and Miller, J. T., *Appl. Catal. A: Gen.* **166**, 293–299 (1998).
36. Mishin, V., Klyachko, A. L., Brueva, T. R., Nissenbaum, V. D., and Karge, H.G., *Kinet. Catal.* **34**, 5, 835–840 (1993).